Control of Switched-Mode Boost Converter by Using Classical and Optimized Type Controllers

Arnab Ghosh*, Subrata Banerjee**

** Research Scholar, Department of Electrical Engineering, National Institute of Technology, Durgapur-713209, India. (e-mail: aghosh.ee@gmail.com)*
*** Professor, Department of Electrical Engineering, National Institute of Technology, Durgapur-713209, India. (e-mail: bansub2004@yahoo.com)*

Abstract: In this paper design and implementation of Type controllers have been performed by using *k-factor* approach and two different optimization techniques Gravitational Search Algorithm (GSA) and Particle Swarm Optimization (PSO) for obtaining better stability and performance for a closed loop DC-DC Switched Mode Boost Converter. Boost converter have a *right-half-plane zero* (*non minimum phase* system), so it is difficult for the PID controller to exhibit good performance with *load*, *line variations* and *parametric uncertainty.* The comparative closed-loop performances of a boost converter with classical and optimized Type II/Type III controllers have been produced. Simulations and experimental results are provided to demonstrate the effectiveness of optimized controllers for the proposed converter.

Keywords: Switched-Mode Boost Converter, Non-Minimum Phase System, Type-II & Type-III Controller, Particle Swarm Optimization (PSO), Gravitational Search Algorithm (GSA).

1. INTRODUCTION

The DC-DC power supplies have played important role in every sphere of engineering with wide range of applications from a few tens of watts to several hundreds of megawatts. The most common and essential applications are in personal/laptop computers, cellular phones, Microcontroller/DSP kit, battery chargers, office equipments, spacecraft, power systems devices, telecommunication equipments, high voltage DC transmission, adjustable motor drives and many others (Mohan et al., 2003; Rashid, 2014).

In the early days, the potential dividers (PD's) were used to control and transfer the DC power from one level to another level. Though the operation of PD's is much easier to realize but the conversion is less energy efficient. For improving the energy efficiency, the linear regulators were introduced. The operations of linear regulators are almost similar to the PD's, embedded with load regulation features and the series resistance is replaced by solid state device. In linear regulators the solid state device operates in active zone that causes a significant amount of power losses across it. Due to the presence of larger heat sinks, and line-frequency transformer, the size and the weight of the power supply is bulky in nature and it is not suitable and economical for large power applications where energy efficiency is a major issue. But in Switch-Mode Power Supplies (SMPS) (Mohan et al., 2003; Rashid, 2014) the solid state device works *like* a switch *i.e.* either completely *on* or *off*. When the device is *on i.e.* conducting, large current flows through it with taking almost zero voltage across it. Similarly when the device is *off*, the voltage across the device is high with almost zero current through it. In both the cases the total power losses across the device is almost zero, so there are less conduction losses in switching regulators. So, energy efficiency is very high (extended up to 95%) in switching regulator and those are found wide applications in many fields engineering *like as* electronic goods and gadgets, DC servo drives, electric transportation system, process control plant and robot automated factories, high-voltage DC transmission (HVDC) system, interconnection of photovoltaic and wind-electric systems to the utility grid, critical medical equipments/instruments, defence equipments *etc*.

Over the last decades the technical developments of DC-DC switching regulators are taken place by the introduction of different kinds of controller (Erickson et al., 2001) for achieving fast dynamic responses as well as better reliability and power density. The performance of DC-DC switching converter can broadly be classified into two categories: (a) transient performance, and (b) steady-state performance. The steady-state performance is mainly guided by the converter-topology, structural configuration of energy storage elements and operating frequency of the power supplies. On the other hand, the transient performance of converter is maintained by the control scheme *i.e.* nature of the controllers (Veerachary, 2012). There are several classical controllers *like* PI, PID controllers; have been developed over the years to ensure desired performance of the converter under specific conditions. Some converters *like* boost, buck-boost, and fly-back have a *right-half-plane zero* (*non minimum phase* system) (Ogata, 2010), so it is difficult for the PID controller to exhibit good performance with load, line variations and parametric uncertainty. For this reason *Type-controllers* (Venable, 1983; Reatti et al., 2003; Escobar et al., 2005; Bryant et al., 2006; Lee, 2014; Ghosh et al., 2014; Ghosh et al., 2015) are best suited. In the proposed work, the design of Type controllers have been aimed by using '*k-factor*' approach and then

controller parameters have to be optimized further by using different optimization techniques for obtaining better stability and performance for a DC-DC Switched Mode Boost Converter.

In recent years, the attention of the researchers have been devoted to implement different optimization techniques over the classical (traditional) control approaches for achieving best and optimised performance of the controllers. The optimal controllers are based on certain methods *such as* characteristics and behaviour of biological, molecular, swarm of insects, neurobiological systems *etc*. There is no specific algorithm to achieve the best solution for all optimization problems. Some algorithms give a better solution for some particular problems than others (Rashedi et al., 2009). Here, *Particle Swarm Optimization* (PSO) and *Gravitational search algorithm* (GSA) are used for design the optimal controllers. The *Particle Swarm Optimization* (PSO) (Eberhart et al., 1995; Al Rashidi et al., 2009; Kennedy, 2010; Clerc, 2010) is based on the behavior of a colony of living things, *like* as swarm of insects, flock of birds, or school of fish. The insects, fishes, animals, especially birds *etc.* always travel in a group without crashing each other from their group members by adjusting their positions and velocities from using their group information. Because this method reduces individual effort for searching the food, shelter *etc*. PSO is an evolutionary algorithm (technique) that optimizes the continuos or discrete, linear or nonlinear, constrained or unconstrained, non differentiable functions by iteratively trying to improve the solutions for different parameter values. *Gravitational search algorithm* (GSA) was introduced by (Rashedi et al., 2009). GSA is based on Newtonian law of gravity (Rashedi et al., 2009; Sabri et al., 2013). This algorithm is simple to understand, easy to implement and gives the optimum controller performance. The DC-DC power supplies are required to deliver regulated output voltage with fast dynamical response, low overshoot, minimal steady-state output error, and low sensitivity to the noise. Recent literatures have been reported, based on the applications of different optimized controllers (Beccuti et al., 2005; Poodeh et al., 2007), PSO and GSA based optimized PI, PID controllers for improving the performance of the DC-DC converter (Yousefi et al., 2008; Emami et al., 2008; David et al., 2009; Abdul-Malek et al., 2009; Liu et al., 2010; Tehrani et al., 2010; Altinoz et al., 2010; Jalilvand et al., 2011; Chung et al., 2011; Khare et al., 2013; Dorf et al., 2011; Siano et al., 2014; Duman et al., 2011; Sarkar et al., 2013). The prior researchers worked on the optimized PI, PID controllers, the optimized Type-II/III has not been reported anywhere. All these requirements have to be satisfied both through the correct design of the circuit parameters and components and mostly by the implementation of appropriate control methodologies. So the optimized controllers are the best suited for any application of DC-DC power supplies in terms of several advantages.

The converter is designed and fabricated in laboratory scale and the specifications are given in Table I. The thump rule of the design is strictly followed to obtain the required voltage & power output of the converter. The implementation of the overall closed loop system is performed by utilizing dSPACE real time controller. The schematic diagram of the overall control system which is being implemented is shown in Fig.1.

It is seen (Fig.1) that the converter uses voltage mode controller where the output voltage of the converter is sensed by LEM make Hall effect voltage sensor. The voltage signal from sensor is appropriately conditioned (filtered & scaled) before feeding to the ADC port of dSPACE controller. The overall control system has been implemented in real time platform by using Simulink module. The conditioned digital voltage output from ADC is compared with a reference input; an error signal is generated and is passed through the optimized Type Controllers which in turn generates the modulating signal. This control signal is then compared with the high frequency triangular waveform to produce PWM signal. This PWM output from dSPACE is passed through DAC, Optoisolator and Astable mutivibrator circuit before inputting to the gate of MOSFET switch of Boost converter.

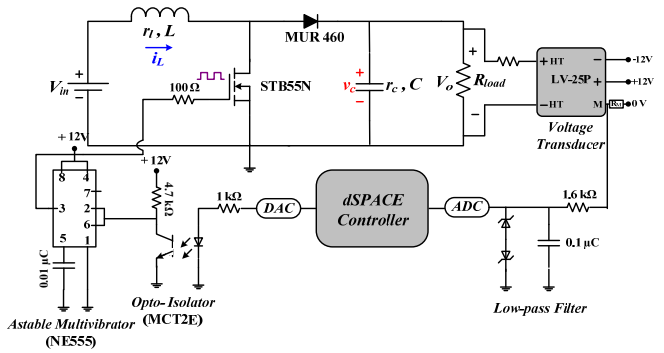

Fig. 1. Schematic diagram of closed-loop operation for boost converter.

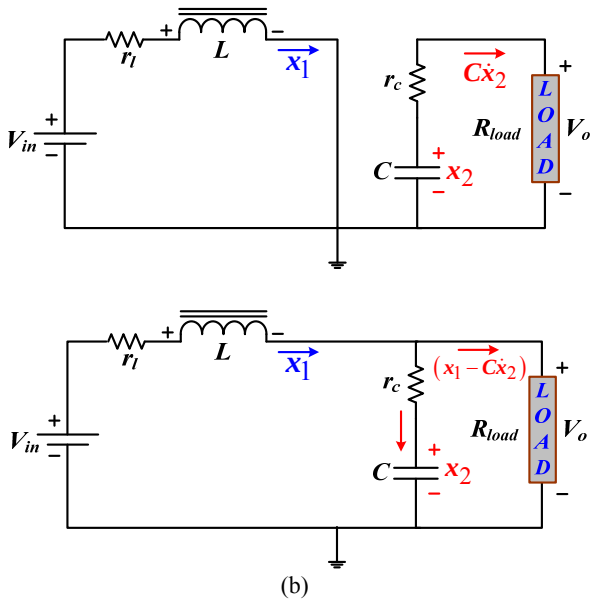

Fig. 2. Equivalent circuit of a boost converter (a) switch on and (b) switch off instant.

2. MODELING OF BOOST CONVERTER

The switching converters are non-linear time varying system. State-Space Averaging (SSA) is an approximation technique that approximates the switching converter as a continuous linear system. In State-Space Averaging method, the corner frequency (f_{corner}) of the output filter to be much smaller than the converter's switching frequency (f_{sw}) (*i.e.* $f_{corner}/f_{sw} << 1$). That implies low output-switching ripple. From the SSA technique, the mathematical modelling can be found from

equivalent circuit model of the converter. The small-signal transfer functions can be derived from the mathematical model of the switching converter. The major advantages of this method are the establishment of a complete converter model with both steady-state and dynamic quantities. (Ang et al., 2005)

Boost converter during switch on condition:

Let, $x_1 = i_L(t)$ = Inductor Current and $x_2 = v_c(t)$ = Capacitor Voltage are two state variables.

Applying kirchoffs law

$$V_{in} - r_l x_1 - L\dot{x}_1 = 0$$
$$or, L\dot{x}_1 = -r_l x_1 + V_{in} \quad (1)$$

Again, $x_2 + r_c C\dot{x}_2 - R_{load}\left(-C\dot{x}_2\right) = 0$

$$or, C\dot{x}_2 = -\frac{1}{R_{load} + r_c} x_2 \quad (2)$$

Therefore, in state space form, one can write

$$\begin{bmatrix} L & 0 \\ 0 & C \end{bmatrix}\begin{bmatrix} \dot{x}_1 \\ \dot{x}_2 \end{bmatrix} = \begin{bmatrix} -r_l & 0 \\ 0 & -\dfrac{1}{r_c + R_{load}} \end{bmatrix}\begin{bmatrix} x_1 \\ x_2 \end{bmatrix} + \begin{bmatrix} 1 \\ 0 \end{bmatrix} V_{in} \quad (3)$$

Therefore, $A_1 = \begin{bmatrix} -\dfrac{r_l}{L} & 0 \\ 0 & -\dfrac{1}{C\left(r_c + R_{load}\right)} \end{bmatrix}, B_1 = \begin{bmatrix} \dfrac{1}{L} \\ 0 \end{bmatrix}$ (4)

Applying KVL, the output equation becomes

$$v_o = R_{load} i_o = -R_{load} i_c; \left(as\ i_o = -i_c\right)$$
$$or, v_o = -R_{load}\left(C\dot{x}_2\right) = -\left(-\frac{R_{load}}{R_{load} + r_c}\right) x_2 \quad (5)$$

Therefore, $v_o = \begin{bmatrix} 0 & \dfrac{R_{load}}{R_{load} + r_c} \end{bmatrix}\begin{bmatrix} x_1 \\ x_2 \end{bmatrix} + [0] V_{in}$ (6)

where, $C_{m1} = \begin{bmatrix} 0 & \dfrac{R_{load}}{R_{load} + r_c} \end{bmatrix}, E_1 = [0]$ (7)

Boost converter during switch off:

A boost converter during switch off condition can be shown in the Fig 2 (b).

Therefore, state-space equations are

$$\begin{bmatrix} L & 0 \\ 0 & C \end{bmatrix}\begin{bmatrix} \dot{x}_1 \\ \dot{x}_2 \end{bmatrix} = \begin{bmatrix} -\left(r_L + \dfrac{R_{load} \times r_c}{R_{load} + r_c}\right) & -\dfrac{R_{load}}{R_{load} + r_c} \\ \dfrac{R_{load}}{R_{load} + r_c} & -\dfrac{1}{R_{load} + r_c} \end{bmatrix}\begin{bmatrix} x_1 \\ x_2 \end{bmatrix} + \begin{bmatrix} 1 \\ 0 \end{bmatrix} V_{in} \quad (8)$$

and output equation is as follows

$$v_o = \begin{bmatrix} \dfrac{R_{load} \times r_c}{R_{load} + r_c} & \dfrac{R_{load}}{R_{load} + r_c} \end{bmatrix}\begin{bmatrix} x_1 \\ x_2 \end{bmatrix} + [0] V_{in} \quad (9)$$

cSo, $A_2 = \begin{bmatrix} -\dfrac{1}{L}\left(r_l + \dfrac{R_{load} \times r_c}{R_{load} + r_c}\right) & -\dfrac{R_{load}}{L\left(R_{load} + r_c\right)} \\ \dfrac{R_{load}}{C\left(R_{load} + r_c\right)} & -\dfrac{1}{C\left(R_{load} + r_c\right)} \end{bmatrix}, B_2 = \begin{bmatrix} \dfrac{1}{L} \\ 0 \end{bmatrix},$

$$C_{m2} = \begin{bmatrix} \dfrac{R_{load} \times r_c}{R_{load} + r_c} & \dfrac{R_{load}}{R_{load} + r_c} \end{bmatrix}, E_2 = [0] \quad (10)$$

Also, $\dfrac{V_o}{V_{in}} = -C_m A^{-1} B$ (11)

$$where, A = DA_1 + (1-D)A_2, B = DB_1 + (1-D)B_2,$$
$$C_m = DC_{m1} + (1-D)C_{m2}$$

The desired transfer function of the power state, $T_p(s)$

$$T_p(s) = \frac{\tilde{v}_0(s)}{\tilde{d}(s)}$$
$$= C_m\left[sI - A\right]^{-1}\left[\left(A_1 - A_2\right)X + \left(B_1 - B_2\right)V_{in}\right] + \left[\left(C_{m1} - C_{m2}\right)X\right] \quad (12)$$

where, I = Identity matrix, D = Duty ratio (Steady-state) and X= State variables (Steady-state).

Finally, output to control transfer function of the Boost plant is

$$T_p(s) = \frac{\tilde{v}_0(s)}{\tilde{d}(s)} \simeq G_{do} \frac{\left\{1 + \left(s/\omega_{z-ESR}\right)\right\}\left\{1 - \left(s/\omega_{z-RHP}\right)\right\}}{\left[1 + \left(s/\omega_o Q\right) + \left(s/\omega_o\right)^2\right]} \quad (13)$$

$$where,\ \text{DC Gain}\left(G_{do}\right) = V_{in}/(1-D)^2;$$
$$\text{Zero due to ESR}\left(\omega_{z-ESR}\right) = 1/\left(r_c C\right)\ \text{rad/sec};$$
$$\text{RHP-Zero}\left(\omega_{z-RHP}\right) = (1-D)^2\left(R_{load} - r_l\right)/L\ \text{rad/sec};$$
$$\text{Natural Frequency}\left(\omega_o\right) = \frac{1}{\sqrt{LC}}\sqrt{\frac{r_l + (1-D)^2 R_{load}}{R_{load}}}\ \text{rad/sec};$$
$$\text{Quality Factor}\left(Q\right) = \omega_o \Big/ \left(\frac{r_l}{L} + \frac{1}{C\left(R_{load} + r_c\right)}\right)$$

Transfer function of boost converter after putting the parameter values (*ref* Table 1).

$$T_{P\_Boost} = \frac{-0.005696s^2 - 0.02559s + 4.983 \times 10^6}{s^2 + 825.3s + 542410} \quad (14)$$

A *right-half plane zero* (RHP) is present in the plant transfer function of the boost-converter (Eqn. (13) & Eqn. (14)) and there is an effect of non-minimum phase due to this RHP.

Table 1. Parameters of Boost Converter.

Circuit Components	Values
Input Voltage V_{in}	5 Volt
Output Voltage V_o	12 Volt
Inductance L	250 μH
Output Capacitance C	1056 μF
Inductor Resistance r_l	10 mΩ
ESR of Capacitor r_c	30 mΩ
Load Resistance R_{load}	25 Ω
Switching Period T	50 μs

3. DESCRIPTION AND DESIGN OF TYPE CONTROLLERS

The design of controllers will play an important factor for maintaining good dynamic performances and regulation of a power supply. In this paper 'Classical Type-II/III' controllers have been used for keeping overall closed loop stability and good dynamic response of the boost converter.

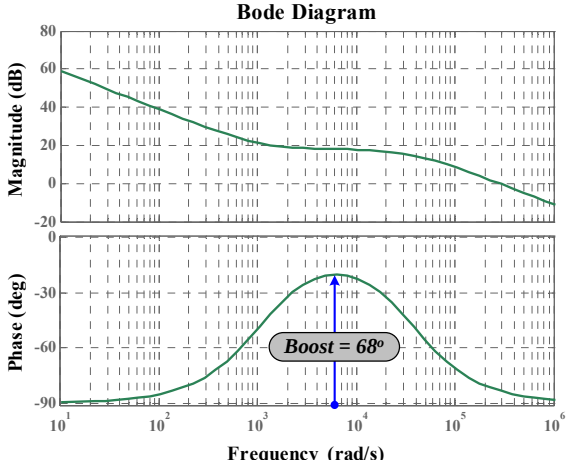

(a)

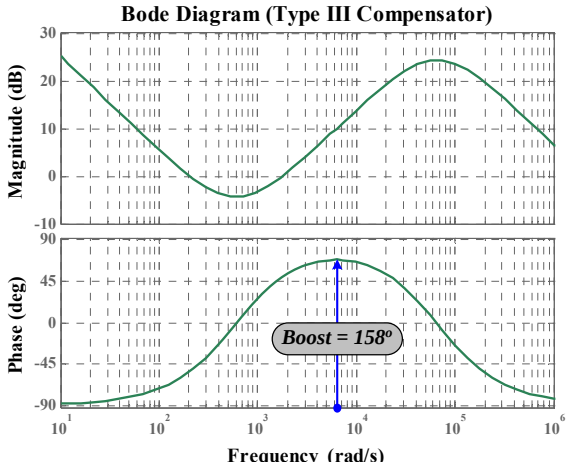

(b)

Fig. 3. The Bode diagram of (a) Type-II and (b) Type-III controller.

3.1. Type-II Controller Design

The "Type-II" controller is one kind of lead controller with a pole at origin. So, this controller provides maximum 90° phase boost with zero steady state error. Even though boost converter having *non-minimum phase* problem, it exhibits a better closed loop performance with a cascaded Type-II controller. With proper tuning of this controller the converter may perform faster response, with minimal overshoots and zero steady-state error (Ghosh *et al*., 2015).

3.1.1. Mathematical Approach

The transfer function of Type-II controller is:

$$T_{c\_II}(s)=\frac{\left(1+\frac{s}{\omega_{z\_II}}\right)}{\left(\frac{s}{\omega_{po\_II}}\right)\left(1+\frac{s}{\omega_{p\_II}}\right)} \tag{15}$$

where, ω_{p_II} and ω_{z_II} are respective pole and zero frequency of Type-II controller.
The magnitude of such transfer function is

$$\left|T_{c\_II}(j\omega)\right|=\frac{\left|1+j\frac{\omega}{\omega_{z\_II}}\right|}{\left|j\frac{\omega}{\omega_{po\_II}}\right|\left|1+j\frac{\omega}{\omega_{p\_II}}\right|} \tag{16}$$

The argument is written as

$$\arg T_{c\_II}(j\omega)=\tan^{-1}\left(\frac{\omega}{\omega_{z\_II}}\right)-\tan^{-1}\left(\frac{\omega}{\omega_{p\_II}}\right)-\frac{\pi}{2} \tag{17}$$

The bode diagram of Type-II controller is shown in Fig. 3 (a) where the pole-zero combination has created a localized *phase boost* of 68° at a certain frequency. The *frequency* where the *maximum phase boost* will be occurred can be obtained by taking derivate of Eqn. (17).

$$\frac{d}{df}\left(\arg T_{c\_II}(j\omega)\right)=\frac{d}{df}\left(\tan^{-1}\left(\frac{f}{f_{z\_II}}\right)-\tan^{-1}\left(\frac{f}{f_{p\_II}}\right)-\frac{\pi}{2}\right)$$
$$=\frac{1}{f_{z\_II}\left(\frac{f^2}{f_{z\_II}^2}+1\right)}-\frac{1}{f_{p\_II}\left(\frac{f^2}{f_{p\_II}^2}+1\right)}=0 \tag{18}$$

To solve the Eqn. (18), the maximum phase *boost* is obtained at the *geometric mean* of the pole and zero frequencies, $f_{\max\_II}=\sqrt{f_{p\_II}f_{z\_II}}$. Generally this geometric mean frequency is considered as crossover frequency (f_{c_II}) of the controller.

3.1.2. Derivation of 'k' in Type-II Controller

The '*k*' is defined as the ratio of the pole frequency to the zero frequency in Type-II controller (Venable, 1983). These pole/zero combinations provide an adjustable phase *boost* from 0° to 90° at the crossover frequency. The relation between '*k*' and the phase *boost* provided by the controller is given by Eqn.(19) (Ghosh et al., 2015):

$$k=\tan\left(\frac{boost}{2}+\frac{\pi}{4}\right) \tag{19}$$

As $k=f_{p\_II}/f_{z\_II}$, the location of pole frequency will be

$$f_{p\_II}=k.f_{c\_II}=\tan\left(\frac{boost}{2}+\frac{\pi}{4}\right)f_{c\_II} \tag{20}$$

and the zero frequency will be derived from

$$f_{z\_II}=\frac{f_{c\_II}}{k}=f_{c\_II}\Big/\tan\left(\frac{boost}{2}+\frac{\pi}{4}\right) \tag{21}$$

Assuming crossover frequency (supposed to be less than the switching frequency) and phase boost, the exact locations of pole/zero can easily be found from Eqn. (20) and Eqn. (21).

3.1.3. Mid-Band Gain Adjustment for the Controller

A Type-II controller is simply combination of *single pole/zero pair* with an *origin pole*. Controller has been described in Eqn. (3) and may be described as follows:

$$T_{c\_II}(s)=\frac{\left(s/\omega_{z\_II}\right)\left(1+\omega_{z\_II}/s\right)}{\left(s/\omega_{po\_II}\right)\left(1+s/\omega_{p\_II}\right)}=\frac{\omega_{po\_II}}{\omega_{z\_II}}\frac{1+\omega_{z\_II}/s}{1+s/\omega_{p\_II}}$$
$$=G_{o\_II}\frac{1+\omega_{z\_II}/s}{1+s/\omega_{p\_II}} \quad (22)$$

In the above expression, the term G_{o_II} is called the mid-band gain and G_{o_II} is equal to $\omega_{po\_II}/\omega_{z\_II}$ where the value of ω_{po_II} depends on the desired gain/attenuation at crossover frequency.

3.1.4. Design Example of Type-II Controller

Let's assume a boost converter with having a gain deficit of -18 dB at selected crossover frequency (f_{c_II}) of 1 kHz. The necessary phase *boost* is 68°. So, the pole can be placed at (*from* Eqn. (20))

$$f_{p\_II}=\tan\left(\frac{boost}{2}+\frac{\pi}{4}\right)f_{c\_II}=\tan\left(\frac{68^o}{2}+45^o\right)\times 1000$$
$$=5.14\text{ kHz} \quad (23)$$

From Eqn. (21) the zero location will be at

$$f_{z\_II}=f_{c\_II}\Big/\tan\left(\frac{boost}{2}+\frac{\pi}{4}\right)=1000\Big/\tan\left(\frac{68^o}{2}+45^o\right)$$
$$=194.38\text{ Hz} \quad (24)$$

So the transfer function of the designed Type-II controller is given by $\frac{1000(s+1221.3)}{s(s+32324)}$.

3.2. Type-III Controller Design

The "Type-III" controller is lead-lead controller with a pole at origin. So, this controller can provide maximum phase *boost* of 180° with *zero steady state error*. Even though the presence of non-minimum phase problem in boost converter, the converter may exhibit the best closed loop performance with a Type-III controller. By the proper tuning of this controller the converter may provide the *fastest response* (better than "Type-II" controller) with minimal overshoots and zero steady-state error (Ghosh *et al*., 2014).

3.2.1. Mathematical Approach

The transfer function of the Type-III controller is as follows:

$$T_{c\_III}(s)=\frac{\left(1+s/\omega_{z1\_III}\right)\left(1+s/\omega_{z2\_III}\right)}{\left(s/\omega_{po\_III}\right)\left(1+s/\omega_{p1\_III}\right)\left(1+s/\omega_{p2\_III}\right)} \quad (25)$$

Now the two zeros have been assumed at same point and similarly the two poles are also presumed same point so the location of *double pole* and *double zero* have been considered at $\omega_{z1\_III}=\omega_{z2\_III}=\omega_{z1,2\_III}$ and $\omega_{p1\_III}=\omega_{p2\_III}=\omega_{p1,2\_III}$.

$$T_{c\_III}(s)=\frac{\left(1+s/\omega_{z1,2\_III}\right)^2}{\left(s/\omega_{po\_III}\right)\left(1+s/\omega_{p1,2\_III}\right)^2} \quad (26)$$

The magnitude of the Type-III controller can be written as

$$\left|T_{c\_III}(j\omega)\right|=\frac{\left|1+j\frac{\omega}{\omega_{z1,2\_III}}\right|\left|1+j\frac{\omega}{\omega_{z1,2\_III}}\right|}{\left|j\frac{\omega}{\omega_{po\_III}}\right|\left|1+j\frac{\omega}{\omega_{p1,2\_III}}\right|\left|1+j\frac{\omega}{\omega_{p1,2\_III}}\right|} \quad (27)$$

The argument of the controller is

$$\arg T_{c\_III}(j\omega)=2\tan^{-1}\left(\omega/\omega_{z1,2\_III}\right)-2\tan^{-1}\left(\omega/\omega_{p1,2\_III}\right)-\frac{\pi}{2} \quad (28)$$

The Bode diagram of Type-III controller is shown in Fig. 3 (b) where the pole-zero combinations create a phase *boost* of 158° at a certain frequency. In this controller the maximum phase *boost* of 180° may be found by changing the poles/zeros locations. The *maximum phase boost* may be obtained by taking the derivate of Eqn. (28) with respect to frequency *f*. Finally the *maximum phase boost* can be obtained at the *geometric mean* of the double zero-double pole frequencies in Type-III controller.

$$f_{\max\_III}=\sqrt{f_{z1,2\_III}f_{p1,2\_III}} \quad (29)$$

This geometric mean frequency is considered as crossover frequency (f_{c_III}) in the Type-III controller.

3.2.2. Derivation of 'k' in Type-III Controller

The '*k*' is defined as the ratio of the double pole frequency to the double zero frequency in Type-III controller (Venable, 1983). These poles-zeros combination provide maximum phase *boost* 180° at the crossover frequency. The relation between '*k*' and the phase *boost* of this controller can be written as follows (Ghosh et al., 2014):

$$k=\left\{\tan\left(\frac{boost}{4}+\frac{\pi}{4}\right)\right\}^2 \quad (30)$$

So the pole location will be in Type-III controller

$$f_{p1,2\_III}=\sqrt{k}.f_{c\_III}=\tan\left(\frac{boost}{4}+\frac{\pi}{4}\right)f_{c\_III} \quad (31)$$

and the zero location can be derived from Eqn. (32)

$$f_{z1,2\_III}=\frac{f_{c\_III}}{\sqrt{k}}=f_{c\_III}\Big/\tan\left(\frac{boost}{4}+\frac{\pi}{4}\right) \quad (32)$$

If the crossover frequency (f_{c_III}) is known with the values of necessary phase *boost*, the exact locations of the double-pole/double-zero may be found from Eqn. (31) and Eqn. (32).

3.2.3. Mid-Band Gain Adjustment for the Controller

The controller of Eqn. (25) may be described as follows:

$$T_{c\_III}(s) = \frac{s}{\omega_{z1\_III}} \frac{\left(1+\omega_{z1\_III}/s\right)\left(1+s/\omega_{z2\_III}\right)}{\left(s/\omega_{po\_III}\right)\left(1+s/\omega_{p1\_III}\right)\left(1+s/\omega_{p2\_III}\right)}$$
$$= G_{o\_III} \frac{\left(1+\omega_{z1\_III}/s\right)\left(1+s/\omega_{z2\_III}\right)}{\left(1+s/\omega_{p1\_III}\right)\left(1+s/\omega_{p2\_III}\right)} \quad (33)$$

Here G_{o_III} is known as *mid-band gain* and $G_{o\_III} = \omega_{po\_III}/\omega_{z1\_III}$. The value of ω_{po_III} depends upon the required gain/attenuation at crossover frequency.

$$\text{Now, } G_{o\_III} = G_{III} \frac{\sqrt{1+\left(\frac{\omega_{c\_III}}{\omega_{p1\_III}}\right)^2}\sqrt{1+\left(\frac{\omega_{c\_III}}{\omega_{p2}}\right)^2}}{\sqrt{1+\left(\frac{\omega_{z1\_III}}{\omega_{c\_III}}\right)^2}\sqrt{1+\left(\frac{\omega_{c\_III}}{\omega_{z2\_III}}\right)^2}} \quad (34)$$

G_{III} is an *assumed gain* at crossover frequency f_{c_III}.

$$\omega_{po\_III} = G_{III}.\omega_{z1\_III} \frac{\sqrt{1+\left(\frac{\omega_{c\_III}}{\omega_{p1\_III}}\right)^2}\sqrt{1+\left(\frac{\omega_{c\_III}}{\omega_{p2\_III}}\right)^2}}{\sqrt{1+\left(\frac{\omega_{z1\_III}}{\omega_{c\_III}}\right)^2}\sqrt{1+\left(\frac{\omega_{c\_III}}{\omega_{z2\_III}}\right)^2}} \quad (35)$$

If double coincident poles/zeros pair has been considered, the formula becomes

$$\omega_{po\_III} =$$
$$= G_{III} \frac{\omega_{z1,2\_III}\left[\omega_{p1,2\_III}^2 + \omega_{c\_III}^2\right]}{\omega_{p1,2\_III}^2 \sqrt{\left(\frac{\omega_{z1,2\_III}}{\omega_{c\_III}}\right)^2 + 1}\sqrt{\left(\frac{\omega_{c\_III}}{\omega_{z1,2\_III}}\right)^2 + 1}} \quad (36)$$

3.2.4. Design Example with a Type III

Let's assume a power supply that has a gain deficit of -10 dB at a 1 kHz selected crossover frequency. The necessary phase boost is 158°. From Eqn. (31) and Eqn. (32), the position of the double pole will be as follows:

$$f_{p1,2\_III} = \tan\left(\frac{boost}{4} + \frac{\pi}{4}\right) f_{c\_III} = \tan\left(\frac{158^o}{4} + 45^o\right) \times 1000$$
$$= 10.38 \text{ kHz} \quad (37)$$

The double zero is placed at

$$f_{z1,2\_III} = f_{c\_III} \Big/ \tan\left(\frac{boost}{4} + \frac{\pi}{4}\right) = 1000 \Big/ \tan\left(\frac{158^o}{4} + 45^o\right)$$
$$= 96.28 \text{ Hz} \quad (38)$$

The gain G at 1 kHz has chosen -10 dB. So the position of the 0-dB crossover pole at

$$f_{po\_III} = G \frac{f_{z1\_III}\left(f_{p1,2\_III}^2 + f_{c\_III}^2\right)}{f_{p1,2\_III}^2 \sqrt{\left(\frac{f_{z1,2\_III}}{f_{c\_III}}\right)^2 + 1}\sqrt{\left(\frac{f_{c\_III}}{f_{z1,2\_III}}\right)^2 + 1}}$$
$$= 29.30 \text{ Hz} \quad (39)$$

So the transfer function of the designed Type-III controller is given by $\frac{3.003\times10^6 (s+605)^2}{s\left(s^2 + 1.31\times10^5 s + 4.26\times10^9\right)}$.

4. PARTICLE SWARM OPTIMIZATION (PSO)

4.1 Overview

Particle Swarm Optimization (PSO) is an evolutionary algorithm (technique) that optimizes the continuos or discrete, linear or nonlinear, constrained or unconstrained, non differentiable functions by iteratively trying to improve the solutions for different parameter values (Dorf et al., 2011; Khare et al., 2013). The PSO is based on the behaviour of a colony of living things, *like* as swarm of insects, flock of birds, or school of fish. The insects, fishes, animals, especially birds *etc.* always travel in a group without crashing each other from their group members by adjusting their positions and velocities from using their group information. Because this method reduces individual effort for searching the food, shelter *etc*. Though particle swarm optimization (PSO) and genetic algorithm (GA) both are population based evolutionary techniques, PSO has better computational efficiency because it has been required less memory space, lesser speed of CPU and less number of parameters to adjust (Khare et al., 2013). But GA and other similar techniques (*like* simulated annealing *etc*.) only work with discrete variables, whereas PSO works with flexibly for discrete as well as continuous systems because it is inherently continuous, so D/A or A/D conversion has not been required (Khare et al., 2013).

4.2 Computational Implementation of PSO

Definition of Objective Function: The definition of *objective function* with typical *performance criteria* is the first step for designing the *PSO* based *Optimized Type-II/III Controllers* with desired specifications and constraints under input step signal. Some important output specifications in the time domain are *overshoot*, *rise time*, *settling time*, and *steady-state error*. Generally, there are four kinds of *performance criteria* (Dorf et al., 2011), such as the Integral Absolute Error (IAE), the Integral of Squared Error (ISE), the Integral of Time weighted Squared Error (ITSE), and the Integral of Time weighted Absolute Error (ITAE). Since ITAE performance criterion provides fastest response with small overshoot for a class of optimization techniques, so $fit_{ITAE}(t)$ is used in this simulation study and is represented by:

$$fit_{ITAE}(t) = \int_0^\tau t\left|e(t)\right| dt \quad (40)$$

where, the upper limit τ is chosen as steady-state value.

A concise idea about the PSO algorithm has been described here for a $\bar{E}$-dimensional search space with n_u particles. Consider the i^{th} particle and the particle can be expressed by a position vector : $S_i = (s_{i1}, s_{i2},\ldots,s_{i\bar{E}})$ and a velocity vector : $V_i = (v_{i1}, v_{i2},\ldots,v_{i\bar{E}})$.

The historical best value of position vector for the i^{th} particle can be described as $pbest_i = (p_{i1}, p_{i2},\ldots, p_{iE})$, and group best can be expressed as $gbest = (p_{g1}, p_{g2},\ldots, p_{gE})$.

The positive constants c_1 and c_2 are the individual (cognitive) and group (social) learning rates, respectively, and r_1 and r_2 are uniformly distributed random numbers in the range [0, 1]. The parameters c_1 and c_2 denote the relative importance of the memory (position) of the particle itself to the memory (position) of the swarm. The values of c_1 and c_2 are usually assumed to be 2 so that c_1r_1 and c_2r_2 ensure that the particles would overfly the target about half the time. The inertia weight constant w has to be chosen carefully for obtaining the optimum result with fast convergence and l denotes the iteration number.

The basic steps of the PSO algorithm are as follows:

Step 1: Initialize the particles of n_u population.
Step 2: Compute the error fitness value for the current position S_i of each particle.
Step 3: Each particle can remember its best position (*pbest*) which is known as cognitive information and that would be updated with each iteration.
Step 4: Each particle can also remember the best position the swarm has ever attained (*gbest*) and is called social information and the value would be updated in each iteration.
Step 5: Velocity and position vector of each particle are modified according to (41) and (42), respectively.

$$V_i^{(l+1)} = wV_i^{(l)} + c_1\eta\left[pbest_i^{(l)} - S_i^{(l)}\right] + c_2r_2\left[gbest^{(l)} - S_i^{(l)}\right] \quad (41)$$

$$S_i^{(l+1)} = S_i^{(l)} + V_i^{(l+1)} \quad (42)$$

Step 6: The iteration stops when maximum number of cycles is reached and the desired solution can be found for the corresponding particle. Otherwise the iterative process repeats.

4.3 Optimization Specifications

The parameters of the Type-II and Type-III controllers are to be optimized using PSO based optimization technique. There are actually four parameters for Type-II controllers, but for optimization three parameters are considered, namely DC gain, one zero and one pole. Similarly for Type-III controller for optimization one DC gain, one pair of zeros and one pair of poles have been considered. In both the cases the pole at origin has not been considered because of fixed location. The flowchart of the optimization process is given in Fig. 5. The routine for Particle Swarm Optimization (PSO) has been written in MATLAB (version R2011a). A swarm of 50 particles characterized by three parameters has been initialized. The controller parameters have been initialized and the values are constrained within a range. Optimized result has been obtained after 100 iterations beyond which significant improvement has not been observed. The values for the PSO parameters are given in Table 2.

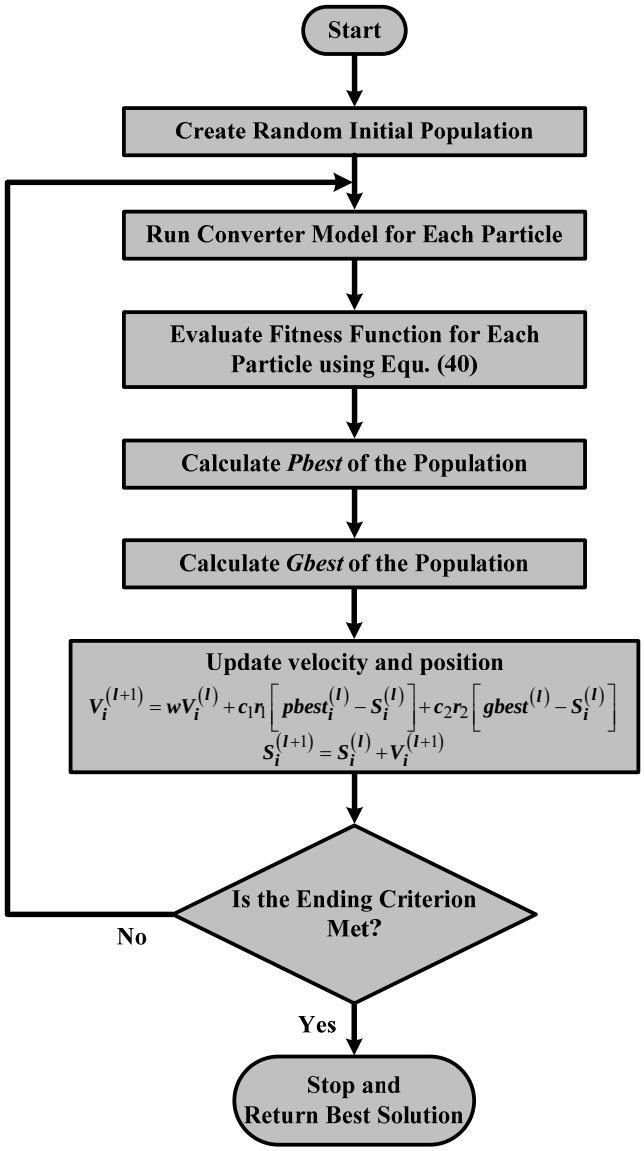

Fig. 4. Flowchart of the Particle Swarm Optimization process.

Table 2. Parameters of PSO Method.

Sl. No.	Parameter	Value
1.	Inertia Weight Constant (w)	0.73
2.	Cognitive Constant (c_1)	1.44495
3.	Group Constant (c_2)	1.44495
4.	Number of Particles (n_u)	50
5.	Number of Iteration (l)	100

5. GRAVITATIONAL SEARCH ALGORITHM (GSA)

5.1 Overview

Gravitational Search Algorithm (GSA), a new optimization algorithm, is based on the law of gravity (Rashedi et al., 2009; Sabri et al., 2013). In this computing technique, the particles are considered as objects and their performance is measured by

their masses. All these objects attract each other by the gravity force, and this force causes a global movement of all objects. Hence, masses cooperate using a direct form of communication, through gravitational force. The heavy masses (which correspond to good solutions) move more slowly than lighter ones. This guarantees the exploitation step of the algorithm. Three kinds of masses are defined in theoretical physics: (a) Active gravitational mass (M_a) is a measure of the strength of the gravitational field due to a particular objet, (b) Passive gravitational mass (M_p) is a measure of the strength of an object's interaction with the gravitational field, and (c) Inertial mass (M_i) is a measure of an object's resistance to changing its state of motion when a force is applied (Rashedi et al., 2009; Sarkar et al., 2013). An object with small inertial mass changes it rapidly.

In GSA, each mass (particle) has four specifications: position, internal mass, active gravitational mass, and passive gravitational mass. The position of mass corresponds to a solution of problem, and its gravitational and inertial masses are determined using a fitness function. In other words, each mass presents a solution, and the algorithm is navigated by properly adjusting the gravitational and inertia masses.

The GSA could be considered as an isolated system of masses. It is like a small artificial world of masses obeying the Newtonian laws of gravitation and motion. More precisely, masses obey the following laws:

a). Law of gravity: Every particle in the universe attracts every other particle and the gravitational force between two particles is directly to the product of their masses and inversely proportional to the square of the distance (R) between them. Rashedi *et al.* used R instead of R^2 because R offered better results than R^2 in all their experimental cases with benchmark functions. Using single exponent instead of double exponent for R causes the departure of the present GSA from exact Newtonian Law of gravitation.

b). Law of motion: The current velocity of any mass is equal to the sum of the fraction of its previous velocity and the variation in the velocity. Variation in velocity or acceleration of any mass is equal to the force acted on the system divided by the mass of inertia.

5.2 Computational Implementation of GSA

Let, the position of the q^{th} particle (masses) among the n_p total number of particle vectors (population) can be explained by:

$$Z_q = (Z_q^1, Z_q^2, Z_q^3, \ldots\ldots Z_q^d, \ldots\ldots Z_q^n) \quad \text{for } q = 1,2,\ldots,n_p \tag{43}$$

where Z_q^d represents the position of q^{th} particle vector in the d^{th} dimension.

In our study each particle vector of the population n_p denotes three parameters or dimension for Type-II controller (Z_q^1= controller gain, Z_q^2= zero location, and Z_q^3= pole location) and five parameters or dimension for Type-III controller (Z_q^1= controller gain, Z_q^2= 1st zero location, Z_q^3= 2nd zero location, Z_q^4= 1st pole location, and Z_q^5= 2nd pole location).

At time't' a gravitational *force* is acting on particle 'q' from particle 'j' can be written as Eqn. (44)

$$F_{qj}^d(t) = G(t)\frac{M_{pq}(t) \times M_{aj}(t)}{R_{qj}(t) + \varepsilon}\left(Z_j^d(t) - Z_q^d(t)\right) \tag{44}$$

where, $G(t)$ is gravitational constant at time t, M_{aj} is the active mass and M_{pq} is the passive mass related to the particles q and j. $\mathcal{E}$ is a small constant, and $R_{qj}(t)$ is the Euclidian distance between two particles q and j.

$$R_{qj}(t) = \left\| Z_q(t) Z_j(t) \right\|_2 \tag{45}$$

In other words, the gravitational constant $G(t)$ is a function of the initial value (G_0) and iteration time t:

$$G(t) = G_0 e^{-\alpha\left(\frac{t}{t_{\max}}\right)} \tag{46}$$

where $t_{\max}$ is the maximum iteration. α is positive constant.
In this algorithm, it is assumed that the total force on particle q, F_q^d is the sum of randomly weighted the force components F_{qj} from other particles at time t in a dimension d:

$$F_q^d(t) = \sum_{j=1, j\neq q}^{n_p} rand_j F_{qj}^d(t) \tag{47}$$

where $rand_j$ is a random number in the interval [0,1].

The technique is used to perform a good compromise between exploration and exploitation is to decrease the number of agents with lapse of iteration number in Eqn. (47). Therefore, only a set of agents with higher masses apply their forces to others but it may because the exploration power and increase the exploration capability. To control exploration and exploitation, only *Kbest* agents will attract each other. *Kbest* is the function of iteration cycle number. *Kbest* is computed in such a manner that it decreases linearly with time and at last iteration the value of *Kbest* becomes 2 % of the initial number of agents. Now, the modified force equation becomes

$$F_q^d(t) = \sum_{j=Kbest, j\neq q}^{n_p} rand_j F_{qj}^d(t) \tag{48}$$

According to the law of motion, the acceleration of q^{th} particle at d^{th} dimension,

$$a_q^d(t) = \frac{F_q^d(t)}{M_{qq}(t)} \tag{49}$$

where M_{qq} is the inertial mass of q^{th} particle.

The velocity ($\hat{h}$) and position updating formulae are given below:

$$\hat{h}_q^d(t+1) = rand_q \times \hat{h}_q^d(t) + a_q^d(t) \tag{50}$$

$$Z_q^d(t+1) = Z_q^d(t) + \hat{h}_q^d(t+1) \tag{51}$$

where $rand_q$ is a uniform random variable in the interval [0,1].

The Gravitational and inertia masses are simply calculated by using Eqn. (53) and (54).

$$M_{aq} = M_{pq} = M_{qq} = M_q, \quad \text{where } q = 1,2,\ldots n_p. \tag{52}$$

$$\hat{m}_q(t) = \frac{fit_q(t) - worst(t)}{best(t) - worst(t)} \tag{53}$$

$$M_q(t) = \frac{\hat{m}_q(t)}{\sum_{j=1}^{n_p} \hat{m}_q(t)} \tag{54}$$

where $fit_q(t)$ represent the fitness value of the particle q at time t, and, $worst(t)$ and $best(t)$ are defined as follows :

$$best(t) = \min_{j \in \{1,2\ldots n_p\}} fit_j(t) \tag{55}$$

$$worst(t) = \max_{j \in \{1,2\ldots n_p\}} fit_j(t) \tag{56}$$

The flow chart of GSA has been given in Fig. 5.

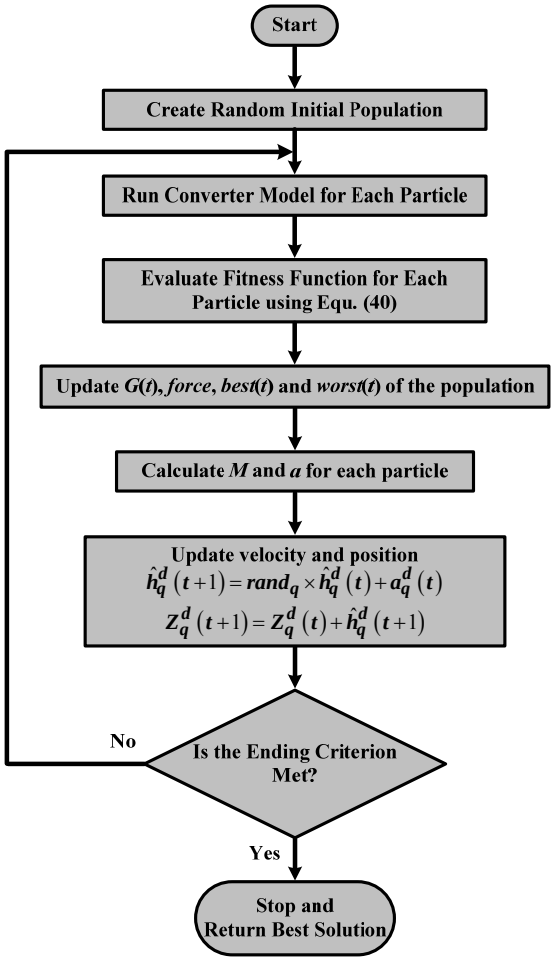

Fig. 5. Flowchart of the GSA optimization process.

5.3 Optimization Specifications

The parameters of the Type-II and Type-III controllers are to be optimized using GSA based optimization technique. There are actually four parameters for Type-II controllers, but for optimization three parameters are considered, namely DC gain, one zero and one pole. Similarly for Type-III controller for optimization one DC gain, one pair of zeros and one pair of poles have been considered. In both the cases the pole at origin has not been considered because of fixed location. The flowchart of the optimization process is given in Fig. 5. The routine for Gravitational Search Algorithm (GSA) has been written in MATLAB (version R2011a). The values for the GSA parameters are given in Table 3:

Table 3. Parameters of GSA method.

Sl. No.	Parameter	Value
1.	Constant (G_0)	3
2.	Constant (α)	2
3.	Number of Particles (n_p)	50
4.	Number of Iteration (t_{max})	100

6. SIMULATION RESULTS AND DISCUSSION

Extensive simulation has been carried out to determine the parameters of Type-II/Type-III controllers using classical and two different optimization techniques (PSO & GSA) so that the closed loop performance of the converter becomes satisfactory. The dynamic performances in terms of step & frequency response of the DC-DC boost converter with Type-II & Type-III controllers have been reported in Fig. 6(a) & (b) and corresponding specifications are given in Table IV (*ref* in Appendix). It is clear that optimized Type-III controllers provide best dynamic response than other controllers. The time response with optimized Type-III controllers shows very fast response with no overshoot and zero steady-state error. It is to be mentioned here that the '*k-factor*' approach is a standard method for design of Type controllers and in the present case it worked well for the closed loop Boost converter. But keeping in view the demand for very fast response of power supply, the controller parameters are further optimized using PSO and GSA method. In the frequency domain analysis it is observed that GSA based Type-III controller generates maximum phase margin (79.3°) and highest gain crossover frequency (7260 rad/sec). Due to have an edge in performance, GSA based technique is considered for practical application. Fig. 6 (c) shows the plot of minimum values of the objective function ($fit_{ITAE}(t)$) versus number of iterations for Type-II and Type-III controller. It is seen that the GSA based Type-III controller produces the least objective function ($fit_{ITAE}(t)$) value than other optimized Type-II and Type-III controllers.

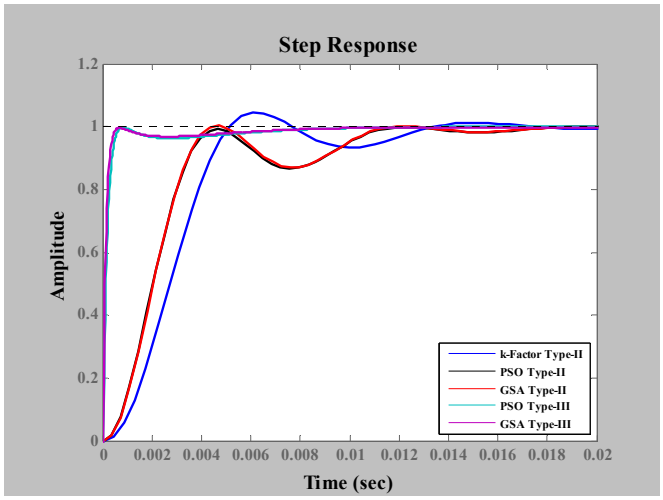

(a)

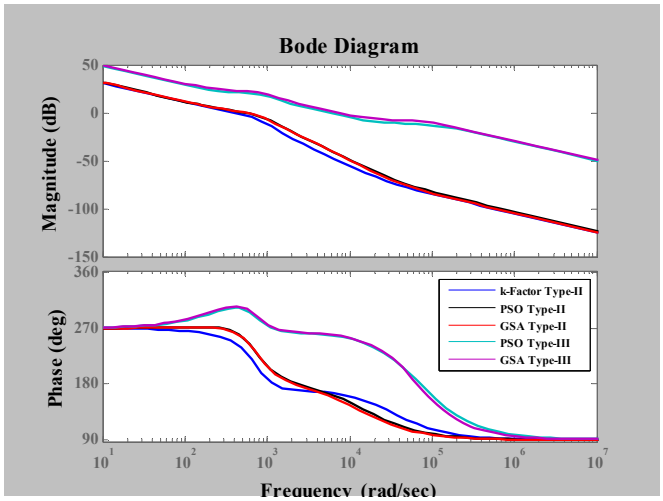

(b)

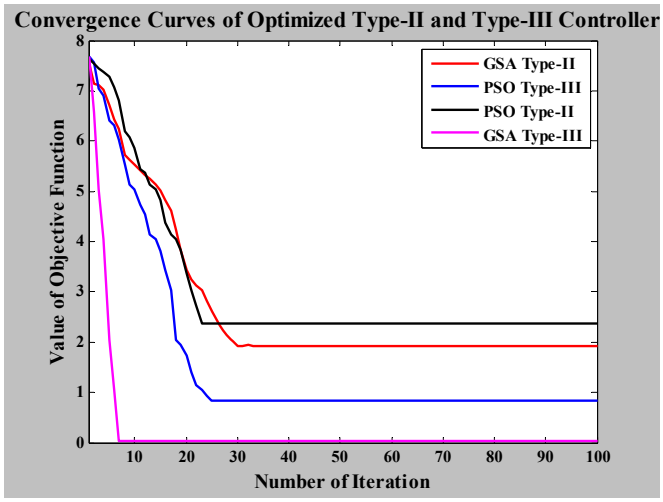

(c)

Fig. 6. (a) Step responses (b) Bode Diagram of closed-loop performances of a boost converter for different Type-II controllers and (c) Convergence curves of objective function ($fit_{ITAE}(t)$) for optimized Type-II and Type-III controller.

7. EXPERIMENTAL RESULTS

The closed loop Boost converter has been implemented practically with the designed controllers utilizing dSPACE based real time system. The overall experimental setup of the system is shown in Fig.7. From the simulation results (Fig. 6), it is clear that for the given converter GSA based optimized Type-III controller exhibits best performance & '*k-factor*' based classical Type-II controller produces relatively worst result while comparing the closed loop performances with different control algorithms. Hence in the implementation part, the above two controllers have been adopted for the closed-loop control of the proposed Boost converter. Fig. 8 (a) & (b) show the dynamic responses of output voltage, coil-current & coil-voltage for the case of optimized GSA controller with positive and negative step change in load voltage respectively. It is clear that in both the cases the output voltage response exhibits faster response without producing any overshoot. The coil-current & coil-voltage dynamics also been observed. The coil current is measured by a current probe with a scale of 100 mV= 1A. The coil voltage appears equal to positive supply voltage during ON time of the switch and the difference between output voltage & input supply voltage comes across the coil during the OFF condition of the switch. As expected, there is overshooting in the output voltage response due to step change in load in case of '*k-factor*' approach (Fig. 8(c)).

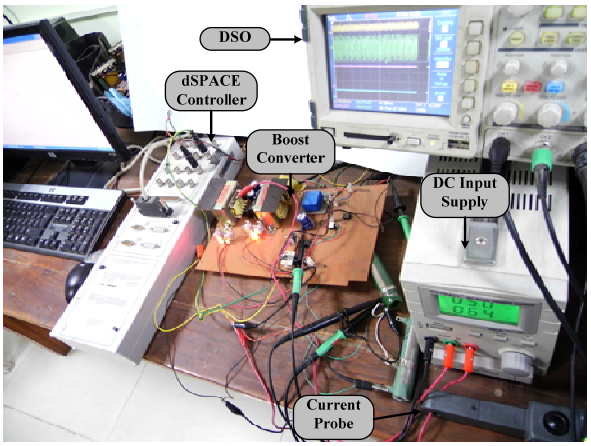

Fig. 7. Overall experimental setup.

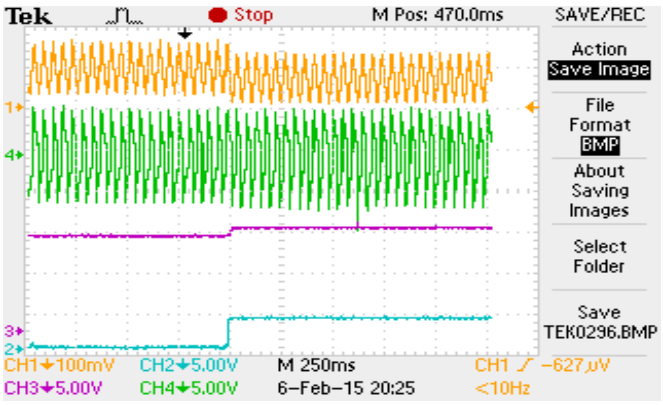

(a)

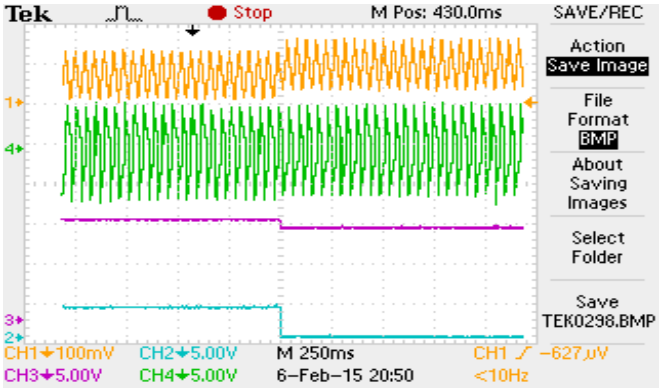

(b)

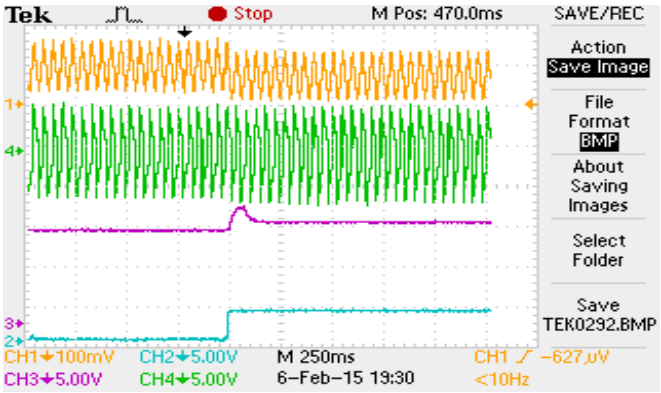

(c)

Fig. 8. Transient response with (a) positive step (b) negative step load disturbance with GSA Type-III controller and (c) Transient response with step load disturbance with '*k-factor*' Type-II controller. [where Ch1: Inductor Current, Ch2: Load Disturbance, Ch3: Load Voltage and Ch4: Inductor Voltage]

8. CONCLUSIONS

In this work the closed loop performances and the comparative analysis for classical and optimized Type-II/III controllers for the Boost Converter have been studied both in simulation and experimentation. It may be concluded that the GSA based optimized Type-III controller exhibits the best closed-loop performance, highest system bandwidth and largest margin of stability. So GSA based optimized Type-III controllers may be used for the design and implementation of Switch Mode Power Boost converter to improve the overall closed loop stability and performance. The proposed control algorithm though applied for lower rated converter, but it may be applicable for higher rating also.

REFERENCES

Abdul-Malek, M. A. and Abido, M. A.(2009). STATCOM based controller design using Particle Swarm Optimization for power system stability enhancement. *IEEE International Symposium on Industrial Electronics* (ISIE 2009), 1218-1223.

Al Rashidi, M.R. and El-Hawary, Mohamed E. (2009). A survey of particle swarm optimization applications in electric power systems. *IEEE Transactions on Evolutionary Computation*, 13 (4) 913-918.

Altinoz, O. T. and Erdem, H. (2010). Evaluation function comparison of particle swarm optimization for buck converter. *IEEE International Symposium on Power Electronics Electrical Drives Automation and Motion* (SPEEDAM), 798-802.

Ang, S., and Oliva, A. (2005). *Power-switching converters*, CRC press.

Beccuti, A. G., Papafotiou, G. and Morari, M. (2005). Optimal control of the boost DC-DC converter. *44th IEEE Conference on Decision and Control and European Control Conference* (CDC-ECC'05), 4457-4462.

Bryant, B. and Kazimierczuk, M. K. (2006). Voltage loop of boost PWM DC-DC converters with peak current-mode control. *Transactions on Circuits and Systems I: Fundamental Theory and Applications*, 53 (1) 99-105.

Chung, I. Y., Liu, W., Schoder, K. and Cartes, D. A. (2011). Integration of a bi-directional dc–dc converter model into a real-time system simulation of a shipboard medium voltage dc system. *Electric Power Systems Research*, 81 (4), 1051-1059.

Clerc, M. (2010). *Particle swarm optimization*, Vol. 93, John Wiley & Sons.

David, R. C., Radac, M. B., Preitl, S., and Tar, J. K.(2009). Particle swarm optimization-based design of control systems with reduced sensitivity. *IEEE 5th International Symposium on Applied Computational Intelligence and Informatics* (SACI'09), 491-496.

Dean Venable, H. (1983). The k-factor: A New Mathematical Tool for Stability Analysis and Synthesis. *Proceedings of Powercon 10*, CA.

Dorf, R. C., and Bishop, R. H. (2011). *Modern control systems*, Pearson.

Duman, S., Maden, D., and Guvenc, U. (2011). Determination of the PID controller parameters for speed and position control of DC motor using gravitational search algorithm. *IEEE 7th International Conference on Electrical and Electronics Engineering* (ELECO), I-225.

Eberhart, R. C. and Kennedy, J. (1995). A new optimizer using particle swarm theory. *Proceedings of the sixth international symposium on micro machine and human science*, vol.1, 39-43.

Emami, S. A., Poudeh, M. B. and Eshtehardiha, S. (2008). Particle Swarm Optimization for improved performance of PID controller on Buck converter, *IEEE International Conference on Mechatronics and Automation* (ICMA 2008), 520-524.

Erickson, R. W., and Maksimovic, D. (2001). *Fundamentals of power electronics*, Springer.

Escobar, G., Leyva-Ramos, J., Martinez, P. R., and Valdez, A.A. (2005). A repetitive-based controller for the boost converter to compensate the harmonic distortion of the output voltage. *IEEE Transactions on Control Systems Technology*, 13 (3) 500-508.

Ghosh, A. and Banerjee, S. (2014). Design of Type-III Controller for DC-DC Switch-Mode Boost Converter. *6th IEEE Power India International Conference* (PIICON-2014), pp. 1-6, 5th -7th December 2014, Delhi Technological University, New Delhi, India. (IEEE *Xplore* D.O.I. 10.1109/34084POWERI.2014.7117679)

Ghosh, A. and Banerjee, S. (2015). Design and Implementation of Type-II Compensator in DC-DC Switch-Mode Step-up Power Supply. *3rd International*

Conference on Computer, Communication, Control and Information Technology (C3IT-2015), pp. 1-5, 7th-8th February 2015Academy of Technology, Hooghly, India. (IEEE *Xplore* D.O.I. 10.1109/C3IT.2015.7060164)

Jalilvand, A., Kimiyaghalam, A., Ashouri, A. and Kord, H. (2011). Optimal tuning of PID controller parameters on a DC motor based on advanced particle swarm optimization algorithm. *International Journal on Technical and Physical Problems of Engineering, optimization*, 3 (4) 10-12.

Kennedy, J. (2010). Particle swarm optimization. *Encyclopedia of Machine Learning* (Springer), 760-766.

Khare, A., and Rangnekar, S. (2013). A review of particle swarm optimization and its applications in Solar Photovoltaic system. *Applied Soft Computing*, 13 (5), 2997-3006.

Lee, S.W. (2014). Practical Feedback Loop Analysis for Voltage-Mode Boost Converter. *Application Report* (SLVA633), Texas Instruments.

Liu, C. H. and Hsu, Y. Y. (2010). Design of a self-tuning PI controller for a STATCOM using particle swarm optimization. *IEEE Transactions on Industrial Electronics*, 57 (2), 702-715.

Mohan, N., Undeland, T. M., and Robbins, W. P. (2003). *Power Electronics*, 3rd ed. Wiley, New York.

Namnabat, M., Bayati Poodeh, M. and Eshtehardiha, S. (2007). Comparison the control methods in improvement the performance of the DC-DC converter, *IEEE 7th Internatonal Conference on Power Electronics* (ICPE'07), 246-251.

Ogata, K. (2010). *Modern Control Engineering*, Pearson Education, India.

Poodeh, M. B., Eshtehardiha, S. and Namnabat, M. (2007). Optimized state controller on DC-DC converter. *IEEE 7th Internatonal Conference on Power Electronics* (ICPE'07), 153-158.

Rashedi, E., Nezamabadi-Pour, H. and Saryazdi, S. (2009). GSA: a gravitational search algorithm. *Information sciences*, 179 (13), 2232-2248.

Rashid, M. H. (2014). *Power Electronics – Devices, Circuits and Applications*, Pearson.

Reatti, A. and Kazimierczuk, M. K. (2003). Small-signal model of PWM converters for discontinuous conduction mode and its application for boost converter. *IEEE Transactions on Circuits and Systems I: Fundamental Theory and Applications*, 50 (1) 65-73.

Sabri, N. M., Puteh, M., and Mahmood, M. R. (2013). A review of gravitational search algorithm. *International Journal of Advance. Soft Comput*, 5 (3).

Sarkar, M.K., Banerjee, S., Saha, T. K., and Ghoshal, S. P. (2013). Implementation of GSA based optimal lead-lead controller for stabilization and performance enhancement of a DC electromagnetic levitation system. *Journal of Control Engineering and Applied Informatics*, 15 (3), 11-20.

Siano, P., and Citro, C. (2014). Designing fuzzy logic controllers for DC–DC converters using multi-objective particle swarm optimization. *Electric Power Systems Research*, 112, 74-83.

Tehrani, K. A., Amirahmadi, A., Rafiei, S. M. R., Griva, G. Barrandon, L., Hamzaoui, M., Rasoanarivo, I., and Sargos, F. M. (2010). Design of fractional order PID controller for boost converter based on multi-objective optimization. *14th International Power Electronics and Motion Control Conference* (EPE/PEMC), T3-179.

Veerachary, M. (2012). *Control of Power Electronic Systems – Digital Solutions*, India.

Yousefi, M. R., Emami, S. A., Eshtehardiha, S. and Bayati Poudeh, M. (2008). Particle swarm optimization and genetic algorithm to optimizing the pole placement controller on Cuk converter, *IEEE 2nd International Power and Energy Conference* (PECon 2008), 1461-1465.

APPENDIX.

Table 4. Comparative Study of Closed-loop Performances

PARAMETER	**TYPE-II (k-factor approach)**	**TYPE-II (PSO)**	**TYPE-II (GSA)**	**TYPE-III (PSO)**	**TYPE-III (GSA)**
Maximum Overshoot (M_p)	4.52 %	0 %	0 %	0.047 %	0 %
Rise Time (t_r)	0.0050 sec	0.0047 sec	0.0043 sec	0.000273 sec	0.000245 sec
Settling Time (t_s)	0.0125 sec	0.0108 sec	0.0107 sec	0.000465 sec	0.000437 sec
Steady-State Error (E_{ss})	0	0	0	0	0
Phase Margin (PM)	67.4°	69.7°	70.9°	78°	79.3°
Gain Crossover Frequency (GCF)	391 rad/sec	567 rad/sec	544 rad/sec	6450 rad/sec	7260 rad/sec
Phase Crossover Frequency (PCF)	1210 rad/sec	2380 rad/sec	2380 rad/sec	72900 rad/sec	66500 rad/sec
Controller Gain (G_o)	1000	1243.1556	1014.0845	6.57×10^6	6.08×10^6
Controller Transfer Function (T_c)	$\frac{1000(s+1221.3)}{s(s+32324)}$	$\frac{1243.1556(s+540.9)}{s(s+16540)}$	$\frac{1014.0845(s+555.56)}{s(s+14084.50704)}$	$\frac{6.57\times10^6(s+524.7)^2}{s(s+7.308\times10^4)^2}$	$\frac{6.08\times10^6(s+500.1905)^2}{s(s^2+1.144\times10^5 s+4.44\times10^9)}$
Closed-Loop Stability	Stable	Stable	Stable	Stable	Stable